Int. J. Electrochem. Sci., 10 **(2015)** 6175 - 6186

International Journal of
ELECTROCHEMICAL
SCIENCE
www.electrochemsci.org

Formation of Porous Anodic Film on Titanium in Acid Media Containing Fluoride Ions at Low Over-potentials

O. Concha[1], I.Castañeda[2], R. Guardian[1], A. Marban[1], D. Mayorga[1], K. Cuentas[3], J. Uruchurtu[1], M. Rincon[3], C. Menchaca-Campos[1,]*

[1]Centro de Investigaciones en Ingenieria y Ciencias Aplicadas UAEM, Mexico
[2]Universidad Tecnologica de Zacatecas, Mexico
[3]Instituto de Energias Renovables-UNAM, Mexico
[*]E-mail: cmenchaca@uaem.mx

Received: 25 November 2014 / *Accepted:* 25 May 2015 / *Published:* 24 June 2015

Titanium oxide nanoporous structures have gained interest due to their possible applications, mainly in the fields of biomaterials, solar energy conversion, photoelectrolysis, and photocatalysis. This work presents the porous anodic film electrochemically formed at low over-potentials on titanium in acid media containing fluoride ions. The anodic titanium oxide growth in acid media has been investigated using potentiodynamic, potentiostatic and electrochemical impedance spectroscopy. Nanometric film pores were formed in the presence of fluoride ions and characterization were provided by scanning electron microscope and digital holography. Depending on experimental conditions, they may contribute to the pore formation and anodic over-potentials facilitate fluoride adsorption and film rupture promoting porous anodic film formation on titanium.

Keywords: Titanium, anodic porous film, oxide porous film, electrochemistry, acid, fluoride.

1. INTRODUCTION

Titanium is a noble metal having very high tensile strength and toughness with good corrosion protection properties, due to the formation of an oxide film with semiconducting properties, depending on the environment in which the metal is placed.

Due to its semiconducting properties, titanium oxide (TiO_2) has a variety of applications, mainly in the fields of biomaterials, solar energy conversion, photoelectrolysis and photocatalysis[1-8].

Referring to biomaterial applications titanium and its alloys out perform any other implant material [10, 11], being used as dental implants and parts for orthodontic surgery, joint replacement parts for hip, knee, shoulder, spine, elbow and wrist, bone fixation materials like nails, screws, nuts

and plates, housing device for pacemakers and artificial heart valves, surgical instruments and components in high-speed blood centrifuges [12-14].

In the energy field, titanium thin oxide films of nanoporous structures have gained interest due to their large surface area, high reactivity and catalytic properties and their applications. Titanium alloys present a wide spectrum of microstructures depending upon alloy chemistry and thermo-mechanical processing. Therefore, one can attempt to tailor their properties for a variety of specific requirements and combinations [15-19]. One of the methods used to form titanium oxide nanostructures is anodizing the surface of titanium in an electrolyte containing fluoride ions. This is usually done at high over-potentials, but scarce research information is reported using low over-potentials [20, 21].

The aim of this work is to induce pores over titanium oxide films under different electrochemical conditions to establish the properties for future development of hybrid or composites materials to be used as a template for different applications.

2. MATERIALS AND METHODS.

2.1 Electrode Materials

Titanium foil of 1.5 x 1.5 cm were obtained from grade II titanium sheet of 0.04 cm thickness and accommodated in an epoxy holder exposing an area of 0.7 or 1cm^2 to the electrochemical solution. Before electrochemical anodizing tests, these electrodes were mechanically polished with silicon carbide powder (grade 400 to 1000) and alumina (particle size from 1 and 0.3 μm) to obtain mirror like finishing, rinsed sequentially for 15 minutes in an ultrasonic bath in ethanol, distilled water, and isopropanol. The anodizing experiments were performed in acid solution: 0.5 M H_2SO_4, or H_3PO_4 without and with the addition of 42 g/l NaF. All the experiments were performed at room temperature. Once the test was concluded, the samples were rinsed with distilled water and dried in a N_2 stream, and stored in a desiccator until required for further analysis.

2.2 Electrochemical Tests.

In order to investigate the electrochemical behavior of the growing titanium oxide, low voltage anodization of the mechanically polished Ti electrodes was performed by applying a potentiodynamic polarization from the open circuit potential to 2.0 V, at the scan rate of 60 mV/min carried out in a 3 electrode electrochemical cell arrangement. A graphite rod was used as the counter electrode and a silver/silver chloride as the reference electrode. The cell was connected to an ACM Gill AC Instruments to obtain the polarization, potentiostatic and electrochemical impedance measurements. Potentiostatic curves were obtained at 1 reading per second at an anodic potential during 3600 seconds at around 1500 mV polarization potential. Electrochemical impedance spectroscopy (EIS) measurements were carried with a sweeping frequency range from 20 kHz to 50 mHz with 5 points per decade and a potential perturbation of 10 mV_{rms} at open circuit potential.

2.3 Digital Holography.

In this work the digital holographic microscopy was used as a tool to observe differences in oxide layer grow onto a titanium sample, allowing numerically access to information of not only the amplitude but also the phase related to the object wave field. In digital holography, the holographic interference pattern is optically generated by superposition of object and reference laser beams, which are digitally sampled by a coupled charge device (CCD) camera and transferred to a computer as a number of arrays, avoiding the necessity of chemical film development as used in conventional holography. Titanium samples, after potentiostatic polarization attack, without and with fluoride ions were mounted on the experimental setup at room conditions. This is a modified Mach-Zehnder interferometer; an amplifier, collimated optical beam emitted from a low power He-Ne laser is divided in two equal intensity beams (i.e. reference and object signals). The object signal is focused with a lens and a 4X microscopic objective onto the metallic sample, which reflected the surface image and recaptured by the objective and focused in the CCD sensor. On the other hand the reference signal is directed by some mirrors and focused also to the camera; a digital hologram obtained by the interference between the two beams is stored in a PC. As in this particular case the image is focused in the camera sensor plane without the need to perform numerical propagation at different planes, and only numerical reconstruction is required to obtain a phase map in order to get a 3D reconstruction at different moments. Variations of the oxide layer formed on the titanium sample are obtained and a hologram was captured. The detailed explanation and setup is reported in the literature [22].

2.4 Characterization

Surface examination of the electrodes was accomplished by an Optimus optical microscope, a scanning electron microscopy (SEM) using a LEO VP 1450, with an EDAX attachment for elemental qualitative and semi-quantitative analysis.

3. RESULTS

To reveal the Ti microstructure a Kroll attack (50 ml H_2O; 3 ml HNO_3; 1.5 ml HF) was performed. The original material microstructure consists of recrystallized α phase grains (in the order of 10μm) with low-density hydrides in the grain boundaries [23].

Figure 1. Optical view of Titanium microstructure (100X).

3.1 Electrochemical Measurements.

Figure 2 presents the potentiodynamic polarization curves obtained under different experimental conditions. Free corrosion potentials became slightly more active with the presence of fluoride ions. A passive region is clearly present, being for the acid solutions similar with small peaks or hump at around 1000 mV. The addition of fluoride ions to the phosphoric acid solution increased the passive current density one order of magnitude. For the sulphuric acid solution containing fluoride ions, a consistent increase in the current density after a small passive region within the polarization range is shown, reaching the current density value of the phosphoric acid containing fluoride ions current density curve. A possible pitting potential around -600 mV can be also observed. The presence of fluoride ions appears to disrupt the anodic passive film formed over titanium.

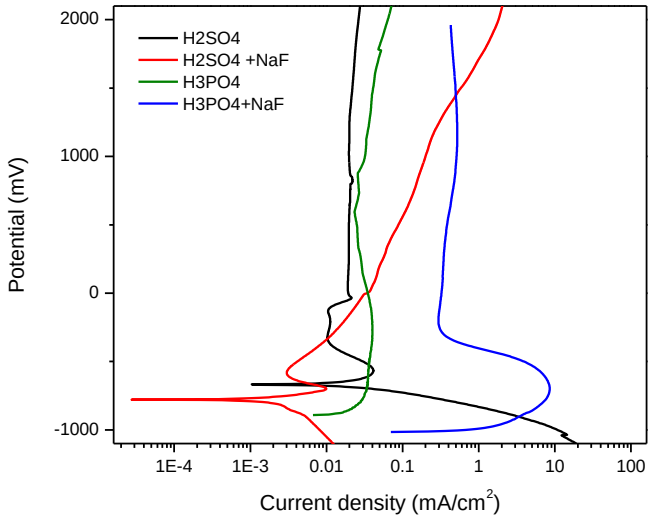

Figure 2. Potentiodynamic polarization curves for titanium in acid media containing fluoride ions.

After electrochemical potentiodynamic polarization characterization was performed, potentiostatic polarization curves without and with fluoride ions addition at 1500 mV, where the current density values are the same, were obtained for one hour of immersion (see figure 3). It can be seen that in the absence of fluoride ions in the solution, the current density value corresponding to the anodic film formation, is in the order of 0.01 mA/cm^2 or less. For the phosphoric acid containing fluoride ions, the current density increased one order of magnitude, and the sulphuric acid and fluoride ions solution, more than two orders. This behavior suggests an increase in porosity of the anodic film under these conditions especially so in sulphuric acid with fluoride ions addition.

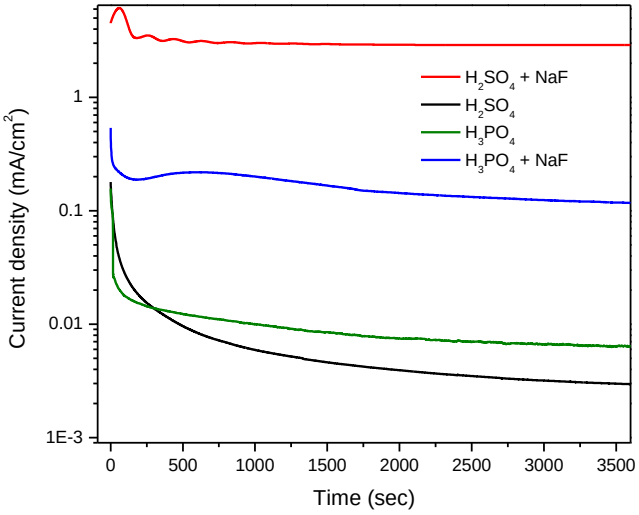

Figure 3. Potentiostatic polarization curves for titanium in acid media containing fluoride ions hold at 1500 mV.

After the potentiostatic polarization hold at 1500 mV for 60 min, afterwards, polarization was suspended, leaving the electrode to relax until reaching the open circuit potential. Afterwards, electrochemical impedance measurements on the electrode in the same solution were made. Figure 4 (a) presents the Nyquist plots obtained for the electrodes in the different electrolytes. In the absence of fluoride ions in the solution, a highly capacitive behavior can be observed while in its presence impedance semicircles are clearly seen.

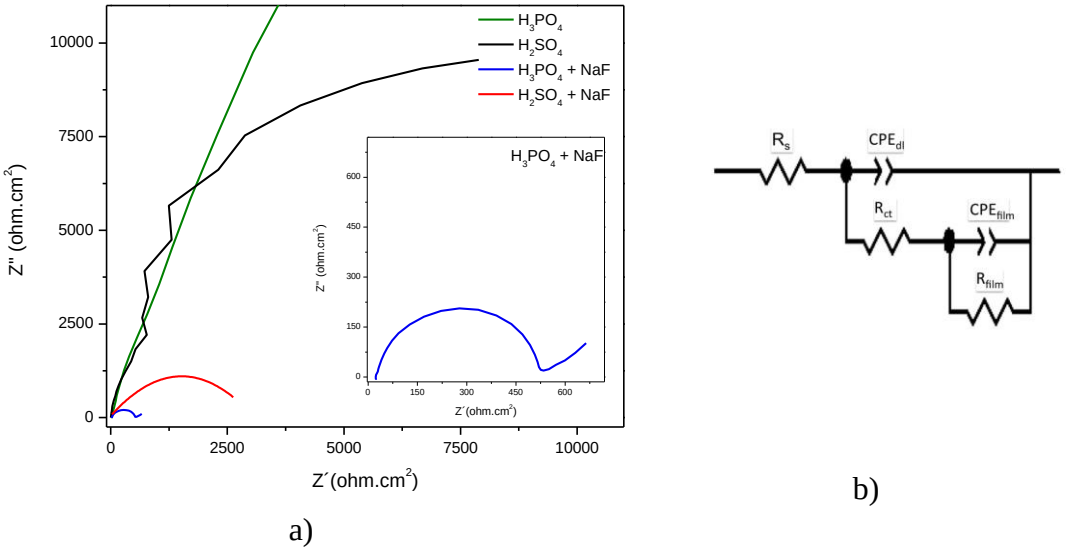

Figure 4. EIS a) Nyquist plot for titanium in acid media containing fluoride ions at open circuit potential and b) equivalent electric circuit.

A mass transport control is suggested from the impedance plots obtained. In figure 4(b) the equivalent circuit used for simulation, to obtain the electrochemical parameters (see table1) is presented [24].

In the presence of fluoride ions the charge transfer decreased as well as the film resistance suggesting an increase in the porosity of the anodic oxide film. Also using a constant phase element, the double layer and film capacitance changes were obtained. Parameter *n*, which is defined by the depression angle in the Nyquist plot, is higher than 0.9 for an ideal capacitive behavior, hardly observed due to surface roughness or heterogeneities that cause uneven current distributions over the electrode surface. When *n* takes lower values and close to 0.5 corresponds to a severe heterogeneity, as with values obtained from simulation, suggesting severe porosity for the anodic film in the presence of fluoride ions. This degree of heterogeneity has been associated to the fractal dimension of the surface determined by electrochemical impedance measurements [25-27]. As the surface of metallic titanium oxide behaves as a dielectric, it is possible to treat the passive layer as a parallel plate capacitor, according to the n_1 and n_2 values obtained in the absence of fluoride ions in solution [28, 29]. In its presence, the lower n_2 values obtained suggest mass transport control through the porous oxide [30, 31].

Table 1. Elements from EIS equivalent electric circuit simulation.

EIS/ solution	R_{sol} □ohm□c m^2)	R_{tc} □ohm□c m^2)	CPE_{dl} (F/cm^2)	n_1	R_{film} □ohm□c m^2)	CPE_{film} (F/cm^2)	n_2
H_2SO_4	29	6356	5.95E-5	0.93	20440	2.68E-5	0.95
H_3PO_4	21	1180	5.74E-6	0.95	29820	1.48E-5	0.81
$H_2SO_4+F^-$	31	251	6.63E-7	1.0	6487	1.75E-5	0.63
$H_3PO_4+F^-$	22	508	2.72E-5	0.86	1590	6.41E-4	0.51

3.2 Digital Holography

As an example of the use of digital holographic microscopy (DHM) based on the phase unwrapping, with the algorithm proposed by Goldstein [22, 32], a digital hologram for titanium in phosphoric acid without and with fluoride ions were obtained and presented in figure 5. The different topography of the anodic films can be clearly seen. The anodic oxide film formed at high polarizing conditions shows defects and cracks all over the surface with a an average thickness around 150 nm up to a maximum height above 300 nm. A notch mark on the sample acting as a visual reference mark to check optical focusing was made and it is shown in the surface profile (figure 5a). Under the fluoride containing solution a porous oxide film is clearly visible (figure 5b) and the morphology observed revealed the differences. The porous oxide layers reached an average thickness around 75 nm and pores up to 200 nm in depth, as can be seen in the oxide profiles presented in figure 5c [22, 33].

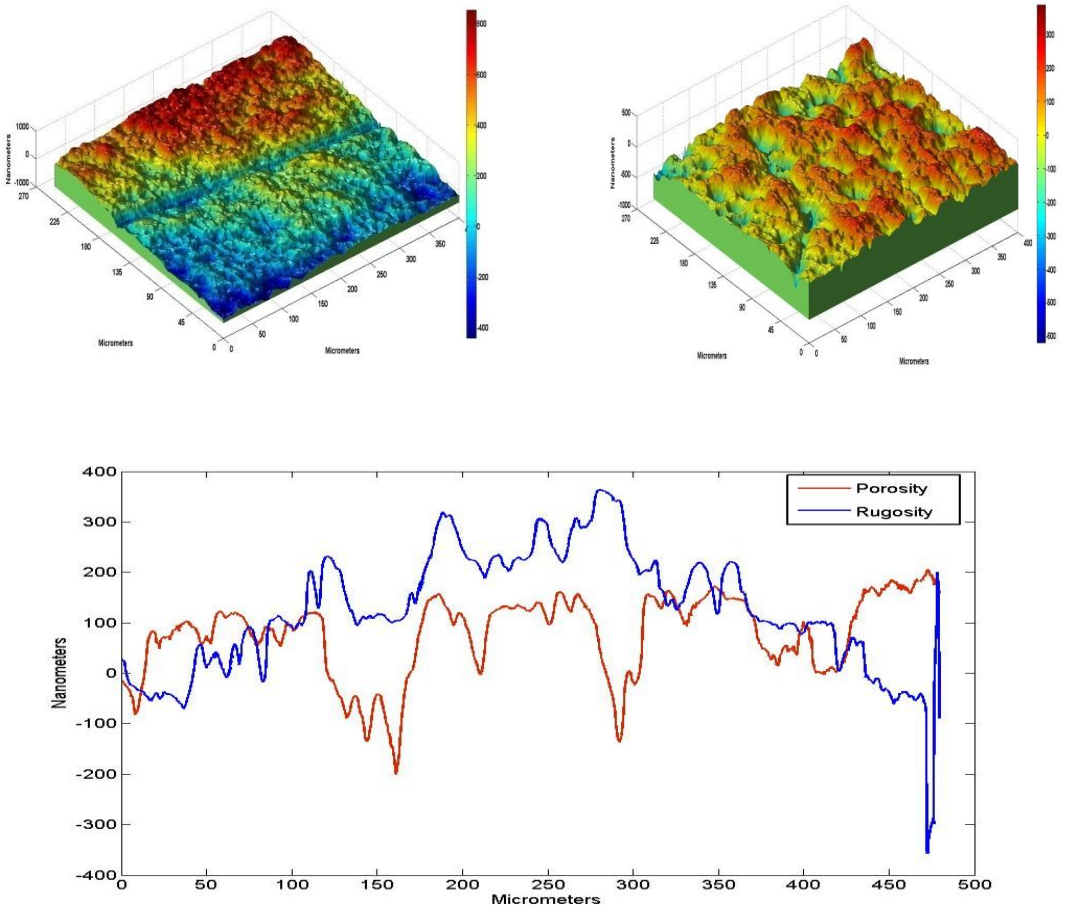

Figure 5. DHM for a) titanium in phosphoric acid hologram, b) titanium in phosphoric acid containing fluoride ions hologram and c) surface profile for both conditions.

3.3 Characterization

Figure 6 presents SEM micrographs showing a) a general view and b) a higher magnification of pores formed in sulphuric acid solution, while c) general view and d) a higher magnification of pores formed in phosphoric acid at high anodic over-potential (1500 mV). Similar pore formation is observed but the sulphuric acid containing fluoride ions in solution, presents a more generalized porous attack appearing shallower, as compared to the phosphoric acid and fluoride ions electrolyte. Pores average diameter is 500 and 300 nm respectively.

Figure 7 were obtained in the SEM for an a) anodic porous film on titanium under phosphoric acid and sodium fluoride solution at high over-potential. An EDAX analysis within the pore (squared marked) was performed. Fluoride is confirmed by the b) fluoride mapping and, c) elemental distribution in weight % where: 55% titanium, 5% sodium, 10% oxygen and 30% fluoride is present.

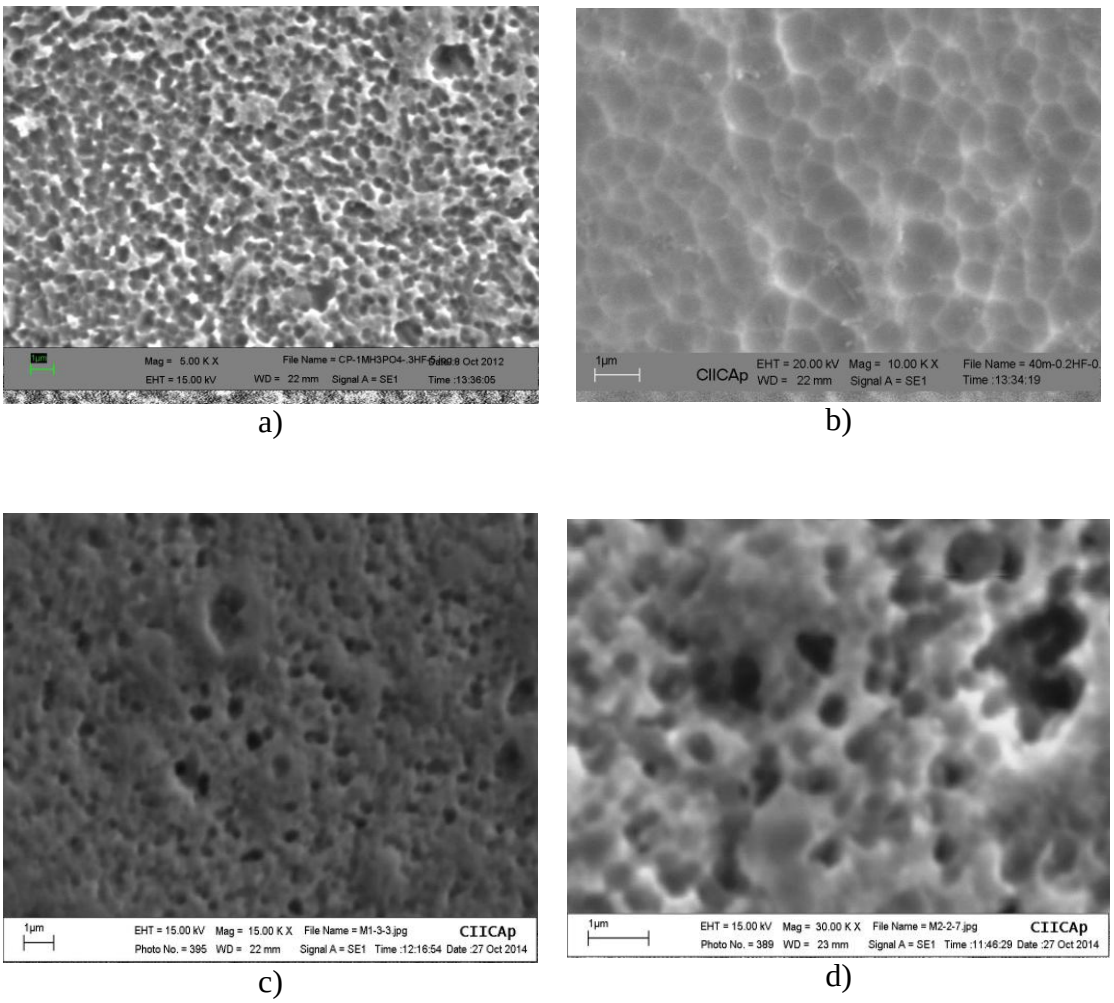

Figure 6. SEM micrographs for titanium in: sulfuric acid containing fluoride ions a) general view b) higher magnification, and phosphoric acid containing fluoride ions c) general view and d) higher magnification.

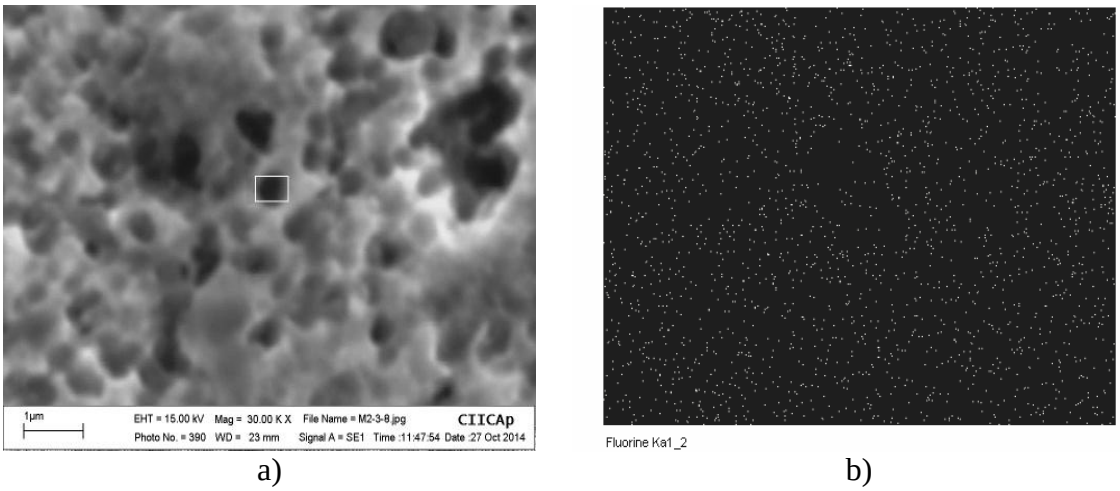

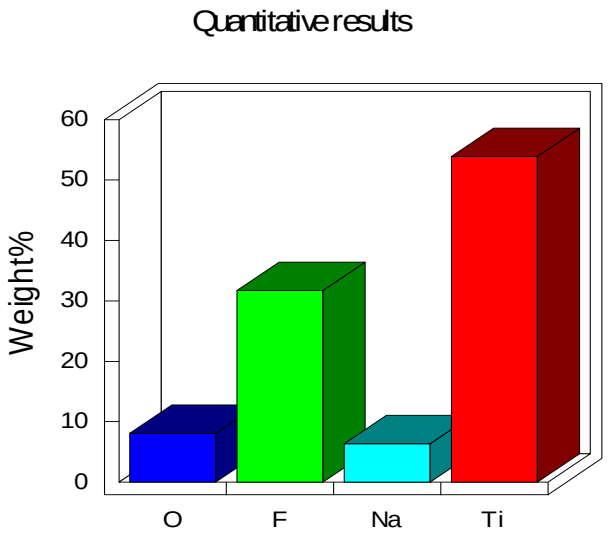

c)

Figure 7. SEM micrograph and EDAX for titanium in phosphoric acid containing fluoride ions a) pore detail analysis, b) fluoride mapping and c) element weight %.

4. DISCUSSION

Titanium possesses high resistance to fatigue and good corrosion behavior. According to the potential-pH Pourbaix diagram, it dissolves at negative active potentials while forming at more noble potentials a protective oxide film (TiO_2) in acid media [34]. As with all active passive metals, in the presence of halide ions in solution, it suffers localized corrosion attack. According to Mazzarolo and coworkers [21], the properties of the porous anodic oxide films formed over titanium present some similarities as well as differences, when compared to aluminum oxide [20, 21].

Beck [35], found that pore diameter and barrier layer thickness depend on the applied potential, while the pore length to the charge passed as long as dissolution at the pore mouth is negligible. The role of the dynamic oxide growth formation is produced by, a combined compressive and/or tensile stresses present in the formed oxide film possibly resulting from an electrostrictive mechanism, that will produce large enough stress to promote breakdown of the passive film [36]. The relief of these stresses is expected to occur at thinner and weakened oxide sites [36-39].

Due to the high electric field across the oxide from polarization, of the order of 10^4 to 10^8 V/m, a corresponding electrostriction pressure, of the order of hundreds of MPa, is present during the growth [21, 37, 38]. Such a stress, combined with ionic migration due to high anodic electrochemical over-potential (+1000 mV, titanium pitting potential) and the addition of anions from the electrolyte, promotes oxide breakdown at local sites [35, 40-44].

The difference between porous oxide growth on titanium and aluminum passive film formation is due to the electrical properties of the growing oxide. Passive film on aluminum presents insulating properties, while titanium anodic films present semiconducting characteristics. As suggested [16, 17,

21], two conduction mechanisms take place: ionic migration of halides and oxygen ions towards the metal and metal ions going into solution; as well as electronic conduction over semiconducting titanium oxide. Ionic migration is responsible for oxide growth, and electronic conduction mainly results in oxygen evolution at the oxide–solution interface [21]. However, unlike aluminum, low or high pH conditions do not promote porous oxide, being necessary the presence of halide ions, as observed in this work [16, 20, 21]. At high electric fields, where ionic migration is possible, low current is associated with electronic conduction for aluminum insulating oxide and comparatively high for titanium semiconducting oxide [41, 45-48].

As Mazzarolo and others [20, 21, 42] suggested, the activation of both mechanisms during oxide growth is also responsible for the gas development within the growing oxide, while fluoride ions migrate faster than oxygen, and form a fluoride-rich layer at the metal–oxide interface [40-42]. This soluble layer is displaced from the metal–film interface to the boundary regions between adjacent pores during the stressed growth [45, 46]. Thus, a soluble layer is continuously generated and chemically dissolved during this process, as suggested in the literature [46-47].

Therefore, under polarizing conditions reaching the so-called “pitting potential” (1000 mV) and beyond [36], in the presence of halide ions such as F^- a twofold effect is produced. First an electrostrictive pressure within the film resulting from the presence of an electric field across it. This field will be higher at the thinner and weakened oxide than the rest of the surface oxide. Second, because of the higher field strength fluoride ions migration is promoted and will be specifically electroadsorbed within the pores, preventing reformation of the film and contributing to its formation [21, 47]. High halide ions concentration within the pores and oxygen evolution are capable of forming pores, similar to the ones observed in this work. Once this is established, at open circuit conditions the mass transfer controls the process and the porous layer is formed [48].

5. CONCLUSIONS

Functionalized titanium is of major importance for practical technological applications. The electrochemical formation of anodic porous oxide film on titanium in acidic solutions containing fluoride ions, at low over-potentials was studied. Porous oxide was produced and characterized in this work. The possibility of controlling the titanium anodic film pore size and growth lies on: the anodic polarizing conditions, the time elapsed during the potentiostatic polarization, the type and concentration of the solution with the presence of halide fluoride ions.

ACKNOWLEDGEMENTS.
The authors wish to thank their academic institutions for the provision of facilities during these works. Also to CONACYT for the student grants and Hector Hugo Gutierrez Payan for holographic images.

References

1. B. O’Regan and M. Gratzel, *Nature*, 353 (1991) 737.
2. G. K. Mor, K. Shankar, O.K. Varghese and C.A. Grimes, *Journal of Materials Research*, 19 (2004)

2989.
3. G.K. Mor, K. Shankar, M. Paulose, O.K. Varghese and C.A. Grimes, *Nano Letters*, 5 (2005) 191.
4. O.K. Varghese, M. Paulose, K. Shankar, G.K. Mor and C.A. Grimes, *J. of Nanoscience and Nanotech*, 5 (2005) 1158.
5. F.E. Osterloh, *Chemistry of Materials*, 20 (2007) 35.
6. M. Ni, M.K.H. Leung, D.Y.C. Leung and K. Sumathy, *Renewable and Sustainable Energy Reviews*, 11 (2007) 401.
7. A. Mills, G. Hill, S. Bhopal, I.P. Parkin and S.A. O'Neill, *J. of Photochem and Photobiology A: Chemistry*, 160 (2003) 185.
8. A. Fujishima, X. Zhang and D.A. Tryk, Surface Science Reports, 63 (2008) 515.
9. S. H. Teoh, *Int. J. Fatigue*, 22 (2000) 825.
10. M. Niinomi, *J. Mech. Behavior of Biomedical Mat.*, 1 (2008) 30.
11. M. Niinomi, *Sci. Tech. Adv. Mater*., 4 (2003) 445.
12. K. Machara, T. Doi, Y. Matsushita, and S. Susaki, *Mater Trans*., 43 (2002) 2936.
13. C. Boehlert, M. Niinomi, and M. Ikedu, *Mat Sci Eng C*, 25 (2005) 247.
14. R. S. Kirby, S. R. Heard, P. Miller, I. Eardley, S. Holmes, and J. Valve, *J. Urol*, 148 (1992) 1192.
15. S. J. Garcia-Vergara, P. Skeldon, G.E. Thompson and H. Habazaki, *Electrochim. Acta*, 52 (2006) 681.
16. J. E. Houser and K. R. Hebert, *Nature Materials*, 8 (2009) 415.
17. K. R. Hebert and J. E. Houser, *J. Electrochem. Soc*., 156 (2009) C275.
18. M. Curioni, E.V. Koroleva, P. Skeldon and G.E. Thompson, *Electrochim. Acta*, 55 (2010) 7044.
19. S. Karimi, N. Fraser, B. Roberts and F. R. Foulkes, *Adv. in Mat. Sci. and Eng.*, 2012 (2012) 22.
20. S. Berger, J. Kunze, P. Schmuki, A. T. Valota, D. J. LeClere, P. Skeldon and G. E. Thompson, *J. Electrochem. Soc.*, 157 (2010) C18.
21. A. Mazzarolo, M. Curioni, A. Vicenzo, P. Skeldonand G.E. Thompson, *Electrochim. Acta*, 75 (2012) 288**.**
22. J. A. Marban Salgado, D. Mayorga Cruz, J. Uruchurtu Chavarin and O. Sarmiento Martinez, *Opt. Pura Apl.*, 46 (2013) 49.
23. G. Domizzi, M.I. Luppo and G. Vigna, *Rev. Materia*, 10 (2005) 150.
24. J. Pan, D. Thierry and C. Leygraf, *Electrochim. Acta*, 41 (1996) 1143.
25. E. Sarmiento, J. G. Gonzalez-Rodriguez, J. Uruchurtu, O. Sarmiento and M. Menchaca, *Int. J. Electrochem. Sci.*, 4 (2009) 144.
26. E. Sarmiento, J. G. Gonzalez-Rodriguez, J. Uruchurtu, O. Sarmiento and C. Menchaca, *Surface and Coatings Tech.*, 203 (2008) 46.
27. M. G. Pujar, T. Anita, H. Shaikh, R. K. Dayal and H. S. Khatak, *Int. J. Electrochem. Sci*., 2 (2007) 301.
28. G. J. Brug, A.L.G. van den Eeden, M. Sluyters-Rehbach and J. H. Sluyters**,** *J. Electroanal. Chem.*, 176 (1984) 275.
29. A. Rahim, *J. App. Electrochem.*, 25 (1995) 881.
30. S. P. Harrington and T. M. Devin, *J. Electrochem. Soc.*, 155 (2008) C381.
31. S. Ait Ali Yahia, L. Hamadou, A. Kadri, N. Benbrahim and E. M. M. Sutter, *J. Electrochem. Soc.*, 159 (2012), K83.
32. R. M. Goldstein, H. A. Zebker and C. L. Werner, *Radio Sci.*, 23 (1998) 713.
33. J. A. Marbán Salgado, J. Uruchurtu-Chavarín and D. Mayorga Cruz, *Int. J. Electrochem. Sci*., 7 (2012) 1107.
34. G.H. Kelsall and D.J. Robbins, *J. Electroanal. Chem. and Interfacial Electrochem.*, 283 (1990) 135.
35. T. R. Beck, *Advances in Localized Corrosion NACE-9*, Eds. H. Issacs, U. Bertocci, J. Kruger and S. Smialowska, NACE, Houston (1990).
36. J.C. Uruchurtu and J.L. Dawson, *Corrosion*, 43 (1987) 19.

37. J. Uruchurtu-Chavarin, *Corrosion*, 47 (1991) 472.
38. J. Uruchurtu, *Advances in Localized Corrosion NACE-9*, Eds. H. Issacs, U. Bertocci, J. Kruger and S. Smialowska, Houston, (1990).
39. G, Okamoto, K. Tachibana, S. Nishiyama and T. Sugita, *Passivity and its Breakdown on Iron and Iron Base Alloys*, NACE, Houston, (1976).
40. A. Valota, D.J. LeClere, P. Skeldon, M. Curioni, T. Hashimoto, S. Berger, J. Kunze, P. Schmuki and G.E. Thompson, *Electrochim. Acta*, 54 (2009) 4321.
41. M. Curioni, F. Roeth, S.J. Garcia-Vergara, T. Hashimoto, P. Skeldon, G.E. Thompson and J. Ferguson, *Surface and Interface Analysis*, 42 (2010) 234.
42. X. Zhou, G.E. Thompson, H. Habazaki, M.A. Paez, K. Shimizu, P. Skeldon and G. C. Wood, *J. Electrochem. Soc.*, 147 (2000) 1747.
43. M. Curioni, E.V. Koroleva, P. Skeldon and G.E. Thompson, *Electrochim. Acta*, 55 (2010) 7044.
44. H. Habazaki, M. Uozumi, H. Konno, K. Shimizu, P. Skeldon and G.E. Thompson, *Corros. Science*, 45 (2003) 2063.
45. L. Iglesias-Rubianes, S.J. Garcia-Vergara, P. Skeldon, G.E. Thompson, J. Ferguson and M. Beneke, *Electrochim. Acta*, 52 (2007) 7148.
46. X. Zhou, G.E. Thompson, P. Skeldon, G.C. Wood, K. Shimizu and H. Habazaki, *Corros. Science*, 41 (1999) 1089.
47. Z. Liu and G.E. Thompson, *J. Mater. Eng. and Performance*, (2014) DOI: 10.1007/s11665-014-1262-7.
48. C. Menchaca-Campos, E. Sarmiento-Bustos and J. Uruchurtu. *Recent Patents on Corrosion Science*, 3 (2013) 12.